Journal of Hazardous Materials 179 (2010) 363–372

Contents lists available at ScienceDirect

Journal of Hazardous Materials

journal homepage: www.elsevier.com/locate/jhazmat

Metal ion removal from aqueous solution using physic seed hull

Masita Mohammad [a], Saikat Maitra [a,*], Naveed Ahmad [a], Azmi Bustam [a], T.K. Sen [b], Binay K. Dutta [c]

[a] Chemical Engineering Department, Universiti Teknologi PETRONAS, 31750, Tronoh, Perak, Malaysia
[b] Chemical Engineering Department, Curtin University, Perth, Australia
[c] Chemical Engineering Program, The Petroleum Institute, P.O. Box 2533, Abu Dhabi, United Arab Emirates

ARTICLE INFO

Article history:
Received 14 September 2009
Received in revised form 3 March 2010
Accepted 4 March 2010
Available online 10 March 2010

Keywords:
Adsorption
Physic seed hull
Cadmium (II)
Zinc (II)
Heavy metal

ABSTRACT

The potential of physic seed hull (PSH), *Jantropha curcas L.* as an adsorbent for the removal of Cd^{2+} and Zn^{2+} metal ions from aqueous solution has been investigated. It has been found that the amount of adsorption for both Cd^{2+} and Zn^{2+} increased with the increase in initial metal ions concentration, contact time, temperature, adsorbent dosage and the solution pH (in acidic range), but decreased with the increase in the particle size of the adsorbent. The adsorption process for both metal ions on PSH consists of three stages—a rapid initial adsorption followed by a period of slower uptake of metal ions and virtually no uptake at the final stage. The kinetics of metal ions adsorption on PSH followed a pseudo-second-order model. The adsorption equilibrium data were fitted in the three adsorption isotherms—Freundlich, Langmuir and Dubinin–Radushkevich isotherms. The data best fit in the Langmuir isotherm indication monolayer chemisorption of the metal ions. The adsorption capacity of PSH for both Zn^{2+} and Cd^{2+} was found to be comparable with other available adsorbents. About 36–47% of the adsorbed metal could be leached out of the loaded PSH using 0.1 M HCl as the eluting medium.

1. Introduction

Heavy metal ions such as cadmium, zinc, copper, lead, nickel, *etc.* are considered as hazardous to the environment due to their toxicity and non-biodegradability even at low concentrations [1,2]. Among these heavy metals, cadmium is potentially hazardous because of its high toxicity and mobility in soil. The permissible limit of cadmium metal ions in wastewater is 2 mg/L [3]. Although zinc is considered as an essential element for life and acts as a micronutrient when present in trace amounts [4], but as recommended by WHO, beyond the permissible limit of 5.0 mg/L in drinking water, Zn^{2+} is also considered to be toxic [5,6].

Cadmium (Cd^{2+}) is released into natural water from different industries like electroplating, cadmium–nickel batteries, phosphate fertilizers, pesticides, mining, pigments, metals and alloys and also sewage sludges [2,6,7]. On the other hand, the main source of Zn^{2+} in wastewater is effluents from metals, chemicals, pulp and paper manufacturing processes, steel works with galvanizing lines, zinc and brass metal works, viscous rayon yarn and fibre production, *etc.* [4].

Various treatment processes such as chemical oxidation, reduction, precipitation, solidification, electrolytic recovery, solvent extraction, membrane separation, ion exchange and adsorption on activated carbon and other adsorbents are some of the wastewater treatment processes for metal ions removal from water bodies [2,8]. However, applications of such methods are sometimes restricted because of technical or economical constraints.

Among these mentioned processes, adsorption is a very effective separation technique and now it is considered as an economical and efficient method for the removal of metal ions present at low concentrations from wastewater [9]. Among the different adsorbents, activated carbon is the most widely used one in a variety of applications [10]. However, considering the cost economics, recent researches have been engaged for the development of alternative low-cost adsorbents using various agricultural, industrial, natural/biological waste materials. Another reason for this interest is the importance of adsorption on solid surfaces in many industrial applications in order to improve the efficiency and the economy of the treatment process. Therefore, it is essential to understand adsorption characteristics, i.e., mechanisms and kinetics of adsorption, because the studies of adsorption kinetics are ultimately a prerequisite for designing suitable adsorption column [11].

In this work, the adsorption potential of an agro waste PSH has been investigated for the removal of Zn^{2+} and Cd^{2+} from their aqueous solution. This study focuses on the influence of solution pH, temperature, particle size, solution–solid ratio and initial metal ions concentration on the metal ions adsorption characteristics of PSH using batch kinetic and equilibrium adsorption experiments. The kinetic adsorption results have been analyzed using both pseudo-first-order and pseudo-second-order kinetics model as well as with intra-particle diffusion model. The isotherm equi-

* Corresponding author. Tel.: +60 14 9021395.
E-mail address: drsaikat_maitra@petronas.com.my (S. Maitra).

0304-3894/$ – see front matter © 2010 Elsevier B.V. All rights reserved.
doi:10.1016/j.jhazmat.2010.03.014

Table 1
Characteristic of the physic seed hull.

Parameter	Value
Sulphur (%)	0.095
Magnesium (%)	0.363
Potassium (%)	1.020
Calcium (%)	1.220
Nitrogen (%)	1.625
Hydrogen (%)	5.785
Carbon (%)	36.623
Oxygen (%)	49.501
Ash (%)	3.768
pH	7.590
pH_{pzc}	2.400
Moisture (%)	8.973
Size distribution (mm)	0.15–1.18
Specific surface area (Multipoint BET-N_2) (m^2/g)	614.01
External Surface Area (t-method) (m^2/g)	89.11
Internal surface area (t-method) (m^2/g)	524.9
Average pore diameter (Å)	30.760
Total pore volume (cm^3/g)	0.4722

librium results were also fitted with Langmuir, Freundlich and Dubinin–Radushkevich isotherm models respectively [12–21].

2. Experiments and methods

2.1. Materials used

The PSH was collected from Bota, Perak, Malaysia. The hull was thoroughly washed with water to remove adhering dirt and soluble components. The washed hull was then oven-dried at 85 ± 10 °C until the weight became constant. The washed and dried materials were crushed and sieved into different size fractions. The hull was sieved using laboratory sieve to obtain sample with the range of 0.15–1.18 mm. The hull was characterized by Fourier transform infra-red (FTIR) Spectroscopy, (Spectrum 2000 Explorer; Perkin Elmer Cetus Instruments, Norwalk, CT) to analyze the organic functional groups present in the adsorbent. The surface morphologies and elemental composition of PSH before and after adsorption of cadmium and zinc were examined with a field emission Scanning Electron Microscope, SEM-EDX (Leo Supra 50 VP, Germany) with gold-coated samples. Elemental composition in terms of C-H-N-S was also measured using CHNS Analyser (CHNS 932, LECO, USA). The surface composition of the sorbent was determined by an energy dispersive X-ray fluorescence (XRF Bruker S4 Pioneer, USA) analysis. The specific surface area and pore size of PSH was measured using BET method by N_2 adsorption isotherm at 77 K using a Quantachrome Autosorb Automated Gas Sorption Instrument, UK. Brunauer–Emmett–Teller (BET) method and Barrett–Joyner–Halenda (BJH) method were used to calculate the surface area and the pore size distribution of PSH. Total volume of pores was calculated at a relative pressure (P/P_0) of 0.99. The zeta potential of PSH was measured using Malvern Zetasizer Nano ZS potentiometer (Malvern Instruments, UK) to assess the surface charge of PSH.

Chemical composition of PSH is given in Table 1. The particle size was measured using Malvern Particle Size Analyser (Model Master Seizer 2000, UK). Standard stock solution of Zn^{2+} and Cd^{2+} was separately prepared by dissolving the required amounts of the metal nitrates in de-ionized water. This stock solution was then diluted to desired concentration levels. The concentrations of Zn^{2+} and Cd^{2+} were measured using double beam flame Atomic Absorption/Flame Emission Spectrophotometer (AAS) Unit (Model Shimadzu AA-660, Japan).

Table 2
Compositions of universal buffer mixture.

0.2 M Na_2HPO_4/mL	0.1 M Citric Acid/mL	pH
20.55	79.45	3
38.55	61.45	4
51.50	48.50	5
63.15	36.85	6

2.2. Adsorption experiment

Studies on the adsorption of metal ions measurements were carried out by batch experiments. For this purpose, 0.4 g of PSH and 100 mL of the metal ions solution were put on a shaker at 160 rpm at a constant temperature of 24 ± 2 °C and a particular solution pH of 6 for a given time. The suspensions were then filtered through a 0.45 μm syringe filter. The filtrate was analyzed using Atomic Absorption Spectrophotometer. The experiments were carried out by varying the initial metal ion concentration (2–50 ppm), particle size (0.15–1.18 mm), contact time (2–240 min), initial solution pH (pH 3–6), amount of adsorbent (0.2–0.6 g) and the temperature (24–60 °C). The pH was adjusted using Universal buffer mixture (0.2 M NH_2HPO_4/mL and 0.1 M Citric acid/mL; Table 2) to avoid the changes on pH due to the present of functional groups at the surface of PSH [22]. The temperature was controlled using water bath laboratory shaker at the range of 24 ± 2 to 60 ± 2 °C. The metal ions concentration retained in the adsorbent phase was calculated using Eq. (1) and the percentage removal of metal ions from solution was calculated using the Eq. (2) (as given in Appendix A).

3. Results and discussions

3.1. Characteristic of the adsorbent

The physico-chemical properties of PSH are presented in Table 1. It is apparent from the table that PSH has a higher internal surface area compared to the external surface area with the average pore diameter of 30.75 Å and total pore volume of 0.4722 cm^3/g as derived from the BET adsorption data. The FTIR spectrum of the PSH is shown in Fig. 1. This spectrum is similar to that of some type of biomass or lignocellulosic materials such as pistachio-nut shell and rockrose [23,24]. Lignin has oxygen functionalities such as phenol, $-SO_3H$ and –COOH groups which provide sites for metal cation exchange [25]. The broad peak at 3409.43 cm^{-1} can be related to overlapping of O–H stretching of H-bonded –OH groups with N–H stretching from primary/secondary amines or amides. The bands appearing at 1647.58 cm^{-1} were related to the formation of oxygen bearing functional groups like highly conjugated C=O stretching in carboxylic groups, and carboxylate moieties, respectively [18]. The peaks at 1049–1647 cm^{-1} indicated the presence of C–H and

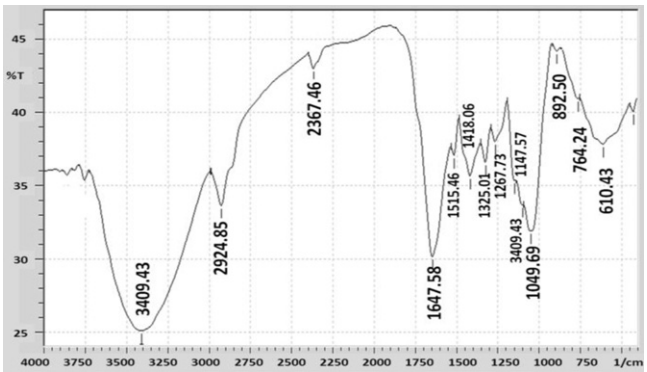

Fig. 1. FT-IR spectrum of PSH.

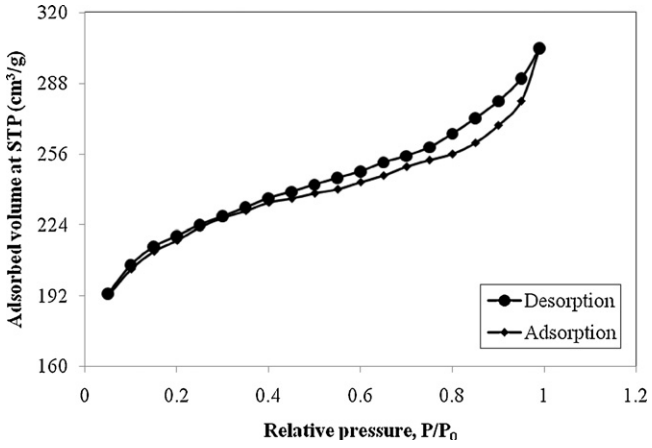

Fig. 2. Nitrogen adsorption–desorption curves of PSH.

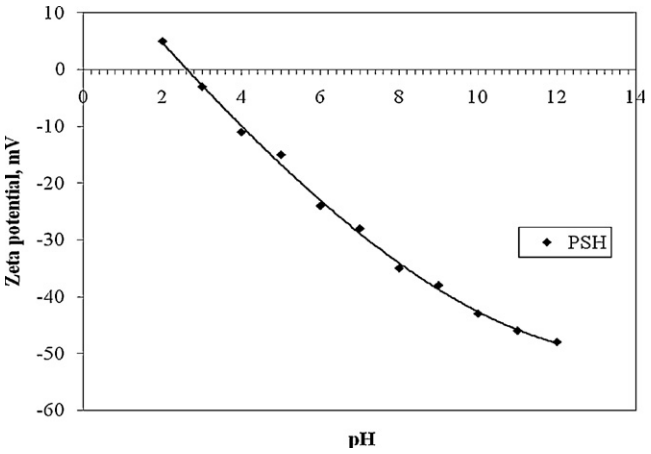

Fig. 4. The zeta potential curves as a function of pH for PSH.

S═O groups, respectively. The C═O and S═O functional groups generally exhibit very high coordination with heavy metals. Hence, the good sorption properties of the PSH towards Cd^{2+} and Zn^{+2} can be attributed to the presence of these functional groups. The adsorbent also exhibited typical stretching vibration of N–H bands present in amides and amines and stretching vibration of C═C at 1647.58, 2924.85 and 2367.46 cm^{-1}. The bands between 2924.85 and 1325.01 cm^{-1} indicated the presence of aliphatic species such as $–CH_3$ and $–CH_2–$. Due to the presence of amino groups (stretching at 3409.43 cm^{-1}), the surface of PSH exhibited a basic nature which was apparent from the increase in pH of the solution soaked with PSH [26]. The amino and amide groups provide additional sites for anchoring metal ions through weak complex formation.

The nitrogen adsorption–desorption curves of PSH is illustrated in Fig. 2. The adsorbed volume increased with an increase in P/P_0, indicating a wider pore size distribution in the adsorbent PSH. This porous adsorbent can be classified as type II isotherm associated with stronger fluid–solid interactions [27]. Fig. 3 shows the pore size distributions of PSH. It appears that PSH contains both micropores and mesopores. From the nature of porosity the adsorption process can be considered as a mesopore dominated capillary condensation phenomena. The strong interaction between adsorbate molecules and pore walls further controls the filling of micropores during adsorption process [27].

Fig. 4 shows the variation of zeta potential of PSH as a function of pH. Zeta potential is the manifestation of surface charge density of the adsorbent. Surface charge density has a significant effect on Cd^{2+} and Zn^{2+} metal ions adsorption on PSH. The pH at the point of zero charge (pH_{pzc} of PSH is 2.4). The pH_{pzc} value is the point at which surface functional groups do not contribute to the pH of the solution. Above this pH value, the surface charge becomes negative and the adsorbent will take up the cations with higher affinity [28].

Scanning electron micrographs along with EDX spectra of PSH as shown in Figs. 5–7 reveal the surface texture and porosity of the sample. The availability of pores and internal surface, which is a requisite for an effective adsorbent, is clearly displayed in the SEM picture of the fresh adsorbent (Fig. 5). The coverage of the surface and the pores by the adsorbed metal ions is displayed in Figs. 6 and 7. The figures further show that after interaction with Cd^{2+} and Zn^{2+} metal ions solution, the peaks corresponding to these ions appeared in the EDX spectra (inset of Figs. 6 and 7) confirming the attachments of these metal ions on PSH surface during adsorption. Some loss in the intensity of Ca^{2+} and Mg^{2+} ions after the adsorption can be related to the translocation between alkaline earth metal ion from the adsorbent surface and the transition metal ions (Cd^{2+} and Zn^{2+}) from the solution during the adsorption process. The change in the morphology of the adsorbent loaded with the metal ions appears very clear from a comparison of Fig. 5 with Figs. 6 and 7. The porous structure that appears in Fig. 5 gets blurred in Figs. 6 and 7 because of adsorption.

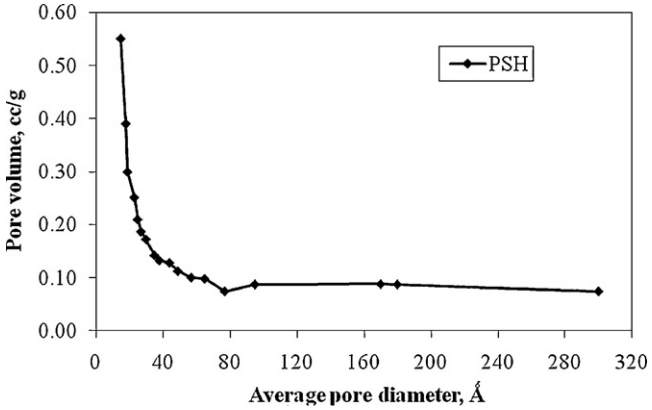

Fig. 3. Pore size distribution of PSH.

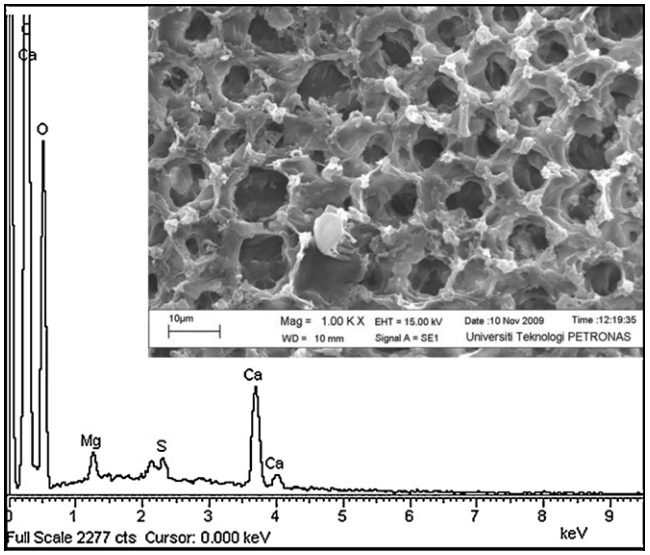

Fig. 5. SEM-EDX image of PSH (300 μm, ×1000mag).

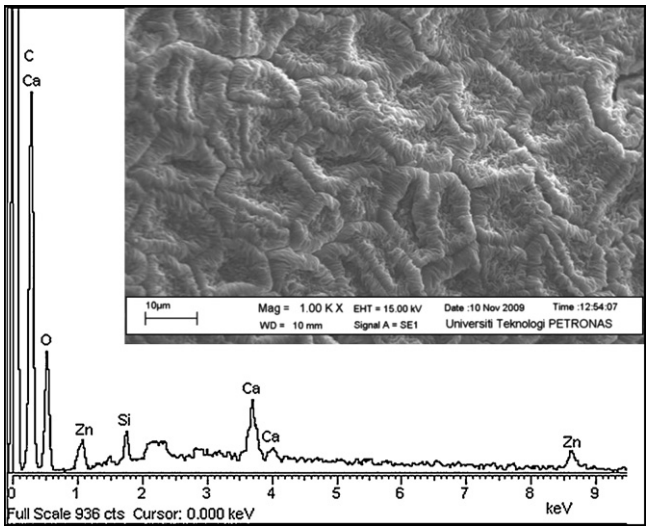

Fig. 6. SEM-EDX image of Zn-loaded PSH (300 μm, ×1000mag).

3.2. Adsorption kinetics

Mechanism of adsorption, particularly the potential rate-controlling step and the transient behaviour of the metal ions adsorption process were analyzed using the Lagergren pseudo-first-order model (Eq. (3)), pseudo-second-order model (Eqs. (4)–(6)) and intra-particle diffusion model (Eq. (7)). In Eq. (3), representing the Lagergren pseudo-first-order model, q_t and q_e represent the amount of metal ion adsorbed (mg/g) at any time t and at equilibrium time, respectively, and K_1 represents the first-order adsorption rate constant (min). Plot of $\log(q_e - q_t)$ versus t gives a straight line for pseudo-first-order adsorption kinetics, which allows computation of the rate constant K_1.

The adsorption data were then analyzed using the pseudo-second-order mechanism (Eqs. (4)–(6)), where K_2 is the pseudo-second-order rate constant (g mg^{-1} min^{-1}). By integrating and applying boundary conditions to Eq. (4), $t = 0$ to $t = t$ and $q = 0$ to $q = q_t$, Eq. (5) was obtained; dq/dt represent the variation in adsorbate uptake with time. The significances of q_t and q_e are similar to that stated before. From a plot of t/q_t versus t the value of the constants K_2 (g mg^{-1} min^{-1}) and q_e (mg/g) were calculated. The

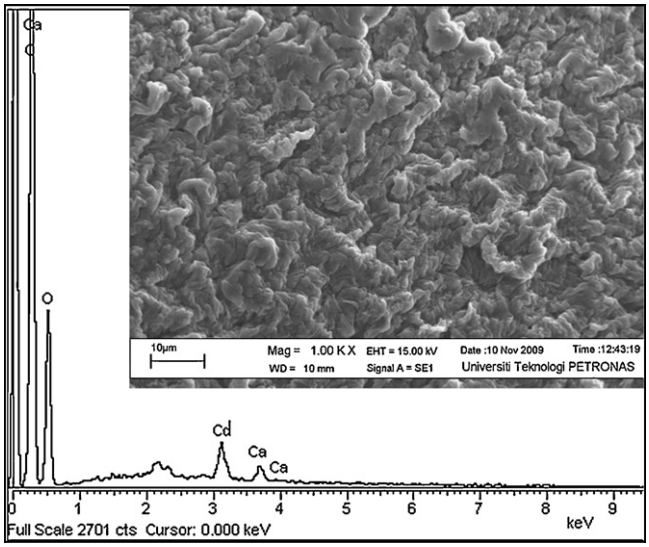

Fig. 7. SEM-EDX image of Cd-loaded PSH (300 μm, ×1000mag).

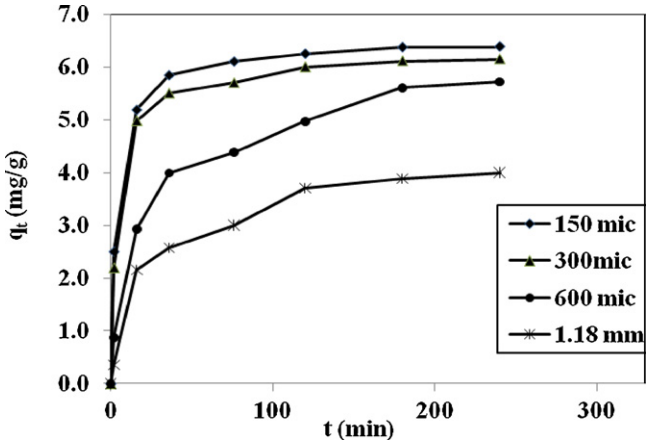

Fig. 8. Effect of contact time on the adsorption of Zn^{2+} at different particle sizes of PSH (size: 0.15, 0.3, 0.6 and 1.18 mm, C_0: 30 ppm, PSH dosage: 0.4 g/100 mL, pH: 6, temp.: 24 °C).

constant K_2 was used to calculate the initial sorption rate, h (the rate of uptake of adsorbent at vanishingly small time, i.e., $t \to 0$) as given by Eq. (6).

All kinetic parameters including the correlation coefficients (R^2) have been calculated and presented in Tables 3 and 4. From the correlation coefficient value, it was evident that the adsorption of Zn^{2+} and Cd^{2+} on PSH followed the pseudo-second-order kinetics. The significance of pseudo-second-order model for the metal ions uptake was that the adsorption followed basically a multi-step chemisorption process [2,5]. Moreover, from Tables 3 and 4 it is apparent that the initial sorption rate (h) and the adsorption (q_e) increased with higher initial metal ions concentration, solution pH and temperature respectively, but decreased with the increase in particle size. Similar type model parameters were obtained by various researchers for a few other absorption systems reported in the literature [5,29]. Generally, adsorption is a mass transfer process where the accumulation of material at the interface of two phases takes place [30]. Therefore increased surface area in smaller particles promoted higher degree of adsorption. The time evolution of uptake as a function of the particle size of PSH for adsorption of Zn^{2+} and Cd^{2+} ion has been shown in Figs. 8 and 9. From the figures it is apparent that higher the particle size, the lower is the percentage adsorption of metal ions. Similar trends with dose and size for other adsorbents was also reported by other workers [30–32].

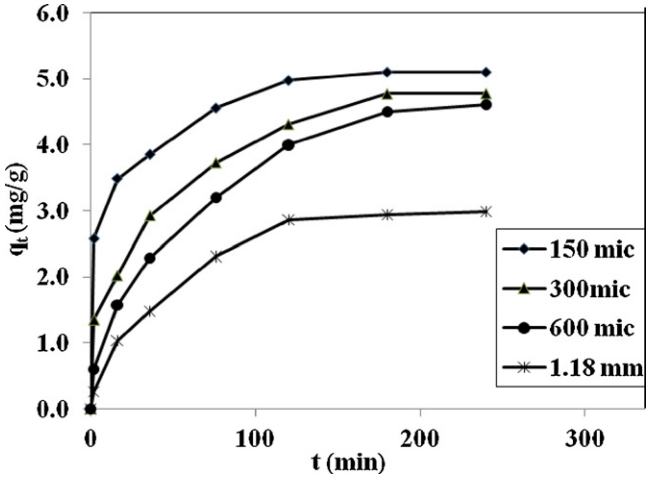

Fig. 9. Effect of contact time on the adsorption of Cd^{2+} at different particle size of PSH (size: 0.15, 0.3, 0.6 and 1.18 mm, C_0: 30 ppm, PSH dosage: 0.4 g/100 mL, pH: 6, temp.: 24 °C).

Table 3
Kinetic parameters for the adsorption of zinc metal ions on physic seed hull.

System parameters	Pseudo-first-order			Pseudo-second-order			
	K_1 (L min^{-1})	q_e (mg/g)	R^2	K_2 (g mg^{-1} min^{-1})	q_e (mg/g)	H (mg g^{-1} min^{-1})	R^2
Initial concentration							
2 ppm (mg/L)	0.0191	0.4776	0.9676	0.2374	0.4684	0.0521	0.9990
5 ppm (mg/L)	0.0223	2.0174	0.8456	0.0737	1.1820	0.1030	0.9984
10 ppm (mg/L)	0.0205	3.4530	0.8587	0.0388	2.3474	0.2136	0.9985
20 ppm (mg/L)	0.0269	18.1970	0.8528	0.0085	4.6533	0.1838	0.9909
30 ppm (mg/L)	0.0235	15.5597	0.8435	0.1665	6.0060	0.2683	0.9930
50 ppm (mg/L)	0.0223	19.7879	0.7801	0.1266	7.8989	0.3787	0.9941
Initial Solution pH							
3	0.0401	2.3410	0.8468	0.0376	1.8278	0.1255	0.9937
4	0.0435	3.4214	0.8979	0.0256	2.1231	0.1155	0.9905
5	0.0412	2.9957	0.9341	0.0300	2.1659	0.1408	0.9945
6	0.0389	3.3963	0.9144	0.0270	2.4195	0.1580	0.9914
Particle Size							
150 μm	0.0456	5.8776	0.8901	0.0522	6.4516	2.1716	0.9997
300 μm	0.0438	6.3052	0.8445	0.0443	6.2150	1.7117	0.9995
600 μm	0.0447	12.4681	0.8052	0.0118	5.9453	0.4171	0.9904
1.18 mm	0.0419	8.2186	0.7695	0.0138	4.2230	0.2453	0.9899
Temperature							
24 °C	0.0428	12.2293	0.7613	0.0119	5.9207	0.4186	0.9909
35 °C	0.0557	16.4097	0.8423	0.0089	6.8540	0.4160	0.9821
45 °C	0.0601	13.5301	0.8810	0.0163	6.9686	0.7916	0.9965
60 °C	0.0488	8.8389	0.9297	0.0223	7.3314	1.1989	0.9985

Increasing temperature has a distinct positive effect on adsorption (Tables 3 and 4) indicating that the process is endothermic [33], an issue that will be quantitatively dealt with later (Section 3.8).

3.3. Effect of amount of PSH on metal ions adsorption

The detailed results of the kinetic experiments with varying adsorbent concentrations are presented in Figs. 10 and 11. From the figures it is clear that the amount of metal ions adsorbed varied with the PSH concentration. The degree of adsorption increased with an increase in the amount of adsorbent in solution and equilibrium was attained within 250 min for the present systems. The experiments were conducted with three different amounts of PSH, 50 mg, 100 mg and 150 mg respectively. The higher degree of adsorption can be related to the increase in adsorption sites with the increase in the adsorbent masses [5,12].

3.4. Effect of initial solution pH on metal ion adsorption

The pH of solutions has been identified as one of the most important parameters governing adsorption on different adsorbents [2,5,7,8,34,35]. Metal species (M (II) = Cd^{2+} or Zn^{2+}) remain present in de-ionized water in the forms of M^{2+}, $M(OH)^{+}$ and $M(OH)_{2(S)}$ [35]. Up to a pH ~ 5.0, the solubility of the $M(OH)_{2(S)}$ is appreciable and therefore, the M^{2+} is the main adsorbate species in the solution [35]. With the increase of the pH value, the solubility of $M(OH)_{2(S)}$ decreases and at pH ~ 10.0, the solubility of $M(OH)_{2(s)}$ is very small. At this pH, the main species in the solution

Table 4
Kinetic parameters for the adsorption of cadmium metal ions on physic seed hull.

System parameters	Pseudo-first-order			Pseudo-second-order			
	K_1 (L min^{-1})	q_e (mg/g)	R^2	K_2 (g mg^{-1} min^{-1})	q_e (mg/g)	H (mg g^{-1} min^{-1})	R^2
Initial concentration							
2 ppm (mg/L)	0.0207	0.4459	0.9374	0.2459	0.4317	0.0458	0.9985
5 ppm (mg/L)	0.0302	2.9758	0.9239	0.0578	1.1071	0.0708	0.9950
10 ppm (mg/L)	0.0104	1.3521	0.9525	0.0251	2.2346	0.1256	0.9957
20 ppm (mg/L)	0.0228	8.3138	0.9077	0.0101	4.1841	0.1763	0.9902
30 ppm (mg/L)	0.0253	13.3444	0.8669	0.2070	4.8309	0.2438	0.9942
50 ppm (mg/L)	0.0223	15.4206	0.8521	0.1587	6.3012	0.2836	0.9935
Initial Solution pH							
3	0.0408	0.9224	0.9000	0.0913	1.1788	0.1269	0.9963
4	0.0419	3.4143	0.8589	0.0246	2.0210	0.1006	0.9885
5	0.0431	2.8701	0.9040	0.0332	2.0496	0.1393	0.9943
6	0.0463	3.9428	0.9008	0.0272	2.2665	0.1399	0.9900
Particle Size							
150 μm	0.0256	3.1857	0.9803	0.0330	5.2083	0.8963	0.9977
300 μm	0.0477	10.1883	0.9034	0.0131	5.0226	0.3293	0.9876
600 μm	0.0451	12.1563	0.8222	0.0079	5.0075	0.1975	0.9724
1.18 mm	0.0368	5.1310	0.8887	0.0123	3.2927	0.1334	0.9791
Temperature							
24 °C	0.0431	11.8468	0.9374	0.0080	4.9776	0.1980	0.9736
35 °C	0.0444	12.1451	0.8930	0.0072	5.7604	0.2399	0.9701
45 °C	0.0438	11.2279	0.9038	0.0108	5.7604	0.3585	0.9879
60 °C	0.0431	13.4958	0.7387	0.0103	6.2972	0.4089	0.9894

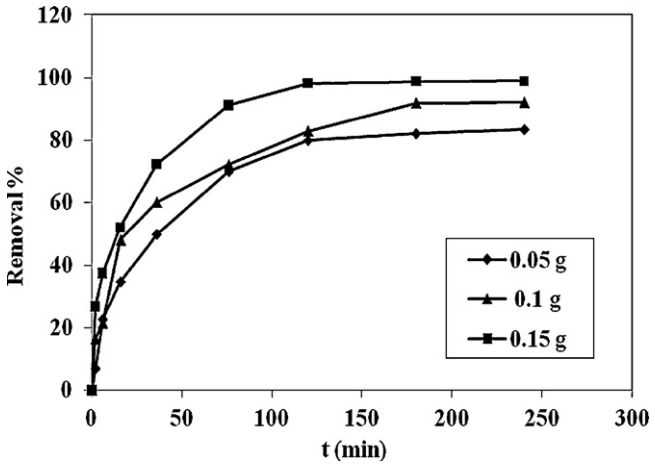

Fig. 10. Effect of various PSH dosages on Zn^{2+} metal ions removal (size: 0.6 mm, C_0: 10 ppm, PSH dosage: 0.2, 0.4 and 0.6 g/100 mL, pH: 6, temp.: 24 °C).

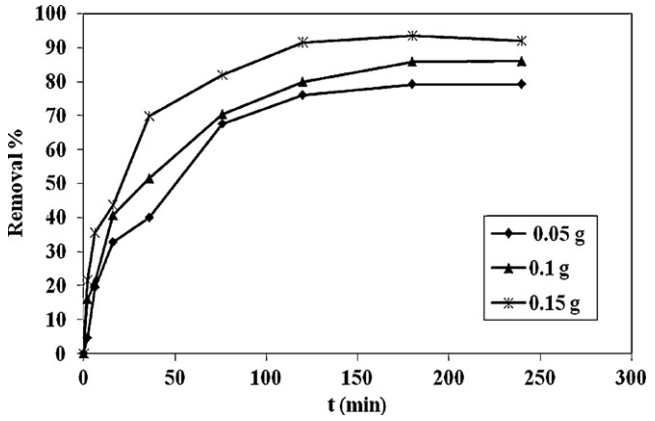

Fig. 11. Effect of various PSH dosages on Cd^{2+} metal ions removal (size: 0.6 mm, C_0: 10 ppm, PSH dosage: 0.2, 0.4 and 0.6 g/100 mL, pH: 6, temp.: 24 °C).

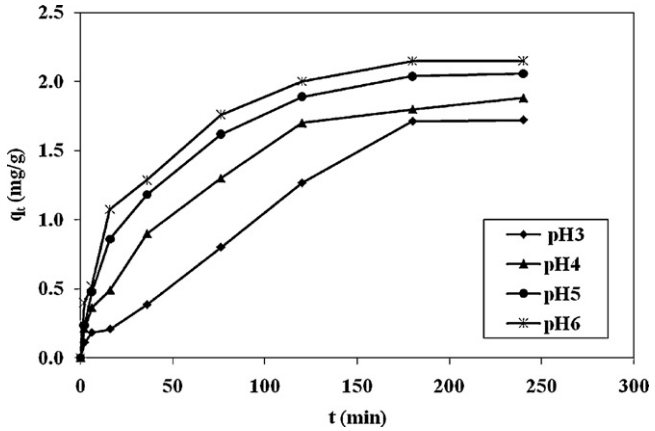

Fig. 12. Effect of contact time on the adsorption of Cd^{2+} onto PSH at different pH (size: 0.6 mm, C_0: 10 ppm, PSH dosage: 0.4 g/100 mL, pH: 3, 4, 5 and 6, temp.: 24 °C).

is $M(OH)_{2(S)}$ [36]. To avoid precipitation of the metal ions, all the experiments were carried out under slightly acidic condition (pH 6.0). The time evolution of the amount of adsorption (q_t) of Cd^{2+} and Zn^{2+} ions by PSH for different initial solution pH is shown in Figs. 12 and 13. The removal of metal ions was found to increase when the solution pH was increased from pH 3.0 to 6.0 for both systems. The maximum uptakes of both metal ions were obtained at about pH of 6.0 within this time period and solution pH range. This

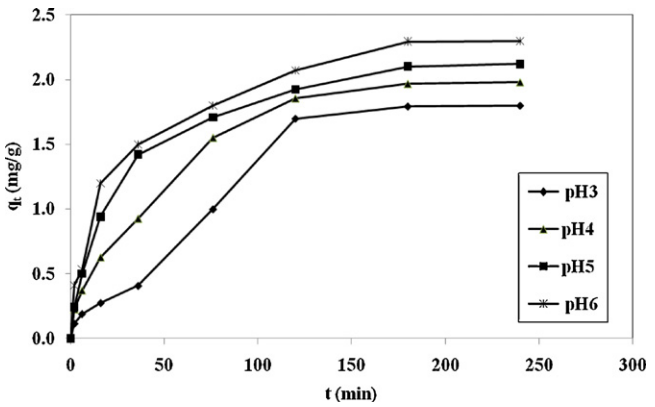

Fig. 13. Effect of contact time on the adsorption of Zn^{2+} onto PSH at different pH (size: 0.6 mm, C_0: 10 ppm, PSH dosage: 0.4 g/100 mL, pH: 3, 4, 5 and 6, temp.: 24 °C).

dependence of metal uptake on pH can be related to the functional groups of the PSH and/or the solution chemistry [8]. PSH primarily contains weak acidic and basic functional groups and carboxyl groups (–COOH) as indicated by the IR absorption spectra. For agro-based adsorbents these groups play important roles for the uptake of metal ions from solution. The minimal adsorption at lower pH may be due to the higher concentration and high mobility of the H^+ ions, which are preferentially adsorbed at the adsorbent surface than other metal ions present in solution [8]. At higher pH, the lower number of H^+ ions in solution along with more negative charge ligands on the adsorbent surface resulted in higher metal ions adsorption. At a pH greater than 3, carboxylic groups were deprotonated acquiring negative charge thereby developing strong attraction with positively charged metal ions.

3.5. Effect of initial concentration on metal ion adsorption

The amount of the adsorption, i.e., mg adsorbate/g of adsorbent increased with increasing contact time at each initial metal ions concentrations and equilibrium was attained within 200 min for both systems. Furthermore, it was observed that the amount of metal ions uptake, q_t (mg/g) increased with the increasing in initial metal ions concentration. Kinetic experiments clearly indicate that adsorption of Zn^{2+} and Cd^{2+} metal ions on PSH followed three-step process, a rapid initial adsorption followed by a period of slower uptake of metal ions and finally no significant uptake [31]. The first step is attributed to the instantaneous utilization of the most readily available active sites on the adsorbent surface (bulk diffusion). Second step, exhibiting additional adsorption, is attributed to the diffusion of the adsorbate from the surface film into the macropores of the adsorbent (pore diffusion or intra-particle diffusion) stimulating further movement of metal ions from the liquid phase onto the adsorbent, PSH surface. The last stage is essentially an equilibrium stage. The following quantitative changes in the three stages are identified from the figures: the metal ion concentration in the residual solution at equilibrium (C_e) for Cd^{2+} for different initial concentrations dropped to 43–58% at the first stage; at the second stage it reduced to 19–40% and at the third stage it dropped down to 14–36%. For Zn^{2+} with different initial concentrations, the ionic concentrations at equilibrium dropped to 24–47% at the first stage, 11–27% at the second stage and 8–23% at the third stage of adsorption. This also shows the higher affinity of the adsorbent towards zinc.

3.6. Intra-particle diffusion model

The intra-particle diffusion model was applied to the experimental data to ascertain the mechanism of the rate-limiting step.

Table 5
Isotherm parameters for the adsorption of Cd^{2+} and Zn^{2+} metal ions on PSH.

Metal ions	Freundlich			Langmuir			Dubinin–Radushkevich			
	k_f (mg/g)	$1/n$ (L/g)	R^2	q_m (mg/g)	k_L (L/g)	R^2	X_m (mol/g)	β (mol^2/kJ^2)	E (kJ/mol)	R^2
Cd^{2+}	0.8157	0.5730	0.9043	11.8906	0.1217	0.9919	0.0246	0.0013	19.6116	0.9089
Zn^{2+}	0.5250	0.5644	0.9190	12.2850	0.2467	0.9958	0.0124	0.0011	21.3201	0.8510

For diffusion controlled adsorption processes, the uptake varies almost linearly with $t^{1/2}$ as shown in Eq. (7) [16], where q_t is the amount adsorbed at time t, K_{id} (mg/g min$^{0.5}$) is the rate constant of intra-particle diffusion and C is the intercept (mg/L). The intra-particle diffusion rate constants were determined from the slope of the linear plot of q_t versus $t^{1/2}$ and values of C were determined from the intercept. The parameter C gives an idea about the thickness (or resistance) of the boundary layer of adsorption [37]. The rate of intra-particle diffusion increased from 0.1074 to 0.2276 mg/g min$^{0.5}$ for Cd^{2+} and 0.0464 to 0.1934 mg/g min$^{0.5}$ for Zn^{2+} with the increasing concentration of both metal ions from 10 to 30 ppm. From the R^2 values (0.9534–0.9993), it is evident that the adsorption followed the intra-particle diffusion model after 36 min of adsorption. The values of C increased from 0.6198 to 1.3022 mg/L for Cd^{2+} and 1.5355 to 2.4136 mg/L for Zn^{2+} with the increase in the initial concentration of Cd^{2+} and Zn^{2+} (10–30 ppm), showing an overall increase in the thickness and the effect of boundary layer.

3.7. Adsorption equilibrium isotherm

Adsorption equilibrium data or isotherms are essential for designing an adsorption system. The measured adsorption equilibrium data have been fitted with Langmuir, Freundlich and Dubinin–Radushkevich isotherm equations within the metal ions concentration range of 2–50 ppm. The Freundlich adsorption isotherm, which assumes that adsorption takes place on heterogeneous surfaces, can be expressed [14,15] by Eq. (8), where q_e is the amount of metal ions adsorbed at equilibrium time, C_e is equilibrium concentration of metal ions in solution. K_f and n are isotherm parameters which indicate the capacity and the intensity of the adsorption respectively [14,15] and can be calculated from the intercept and slope of the plot between $\ln q_e$ and $\ln C_e$.

According to Langmuir model, adsorption occurs uniformly on the active sites of the adsorbent and once an adsorbate occupies a site, no further adsorption can take place at this site. Therefore, Langmuir isotherm equation was tested with the same metal ions concentrations. The linearized form of Langmuir isotherm can be written as Eq. (9). The Langmuir constants, q_m (maximum adsorption capacity, mg/g) and K_L (parameter for Langmuir isotherm related to the affinity of the binding sites and energy of adsorption, L/mg) are calculated from the plot of $1/q_e$ versus $1/C_e$.

The essential characteristics of the Langmuir isotherm can be expressed in terms of a dimensionless constant separation factor R_L that is given by Eq. (10). From this equation, C_0 is the initial concentration of adsorbate (mg/L), and K_L (L/mg) is the Langmuir constant. The value of R_L determines if the adsorption process is favorable or not [38]. The R_L values for the adsorption of Cd^{2+} onto PSH are in the range of 0.1412–0.8043, while for Zn^{2+} onto PSH, the values are in the range of 0.07498–0.6696. The R_L values obtained are found to decrease with the increment of initial metal ions concentration. This indicated that the adsorption of Cd^{2+} and Zn^{2+} on PSH surface is a favorable process and at high initial metal ions concentration, the adsorption is almost irreversible.

The Dubinin–Radushkevich isotherm can be used to describe adsorption on both homogenous and heterogeneous surfaces [19–21]. The linear form of Dubinin–Radushkevich equation are given by Eqs. (11) and (12). In these equations, X_m is the Dubinin–Radushkevich monolayer capacity (mg/g), β is a constant related to sorption energy, and ε is the Polanyi potential which is related to the equilibrium concentration. The constant β gives the mean free energy (E) of adsorption per molecule of the adsorbate when it is transferred to the surface of the solid from infinity in the solution and can be computed from Eq. (13). The magnitude of E is useful for estimating the mechanism of the adsorption process—whether it is chemical ion exchange or physical adsorption. For adsorption of both Cd^{2+} and Zn^{2+} the values of E were more than 16 kJ/mol (Table 5) indicating that the adsorption process were dominated by particle diffusion [39]. Among the three adsorption isotherms tested, the Langmuir isotherm appears to fit the experimental data best as indicated by the high values of the correlation coefficients.

Table 5 presents the fitted Langmuir, Freundlich and Dubinin–Radushkevich isotherm parameters for both Cd–PSH and Zn–PSH systems. Though the uptake of a metal ion depends

Table 6
Langmuir isotherm parameters for the adsorption of Cd^{2+} and Zn^{2+} metal ions on PSH at various conditions.

Parameters	Cd^{2+}			Zn^{2+}		
	q_m (mg/g)	k_L (L/g)	R^2	q_m (mg/g)	k_L (L/g)	R^2
Initial Solution pH						
3	2.1805	0.4027	0.9824	5.9737	0.1778	0.9808
4	6.3052	0.1388	0.9931	9.2166	0.1465	0.9953
5	7.8247	0.1367	0.9970	9.3809	0.1566	0.9944
6	11.9048	0.1215	0.9919	15.1286	0.1876	0.9914
Particle Size						
0.15 mm	13.0548	0.1378	0.9969	16.1031	0.2526	0.9987
0.30 mm	12.7714	0.1213	0.9939	15.5280	0.2246	0.9962
0.60 mm	11.9190	0.1213	0.9919	15.1286	0.1876	0.9914
1.18 mm	3.9246	0.2907	0.9969	4.9579	0.4957	0.9957
Temperature						
24 °C	11.9048	0.1215	0.9919	15.1057	0.1880	0.9914
35 °C	12.1507	0.1393	0.9951	15.2905	0.2650	0.9975
45 °C	15.7233	0.1229	0.9933	16.3399	0.3068	0.9942
60 °C	24.6305	0.0963	0.9918	27.4725	0.2031	0.9899

*Constant parameters: C_0: 5, 10, 20, 30 and 50 ppm, Particle size: 0.6 mm, PSH dosage: 0.4 g/100 mL, pH: 6, temp.: 24 °C.

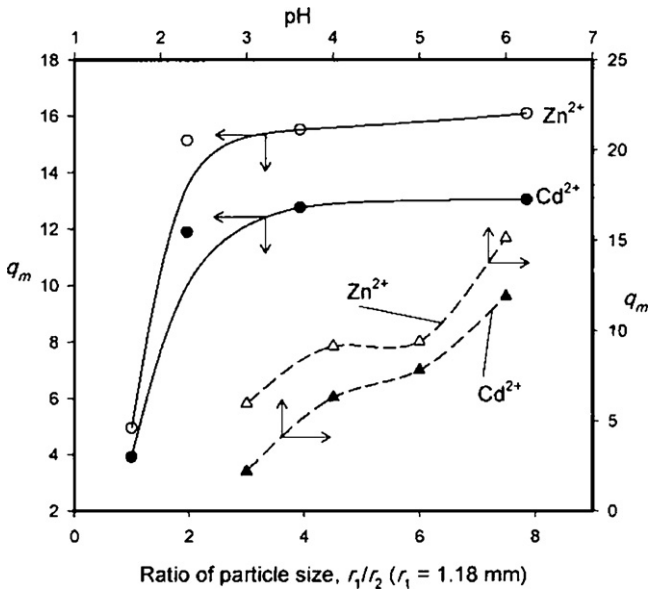

Fig. 14. Variation of maximum adsorption capacity with dimensionless particle size and pH.

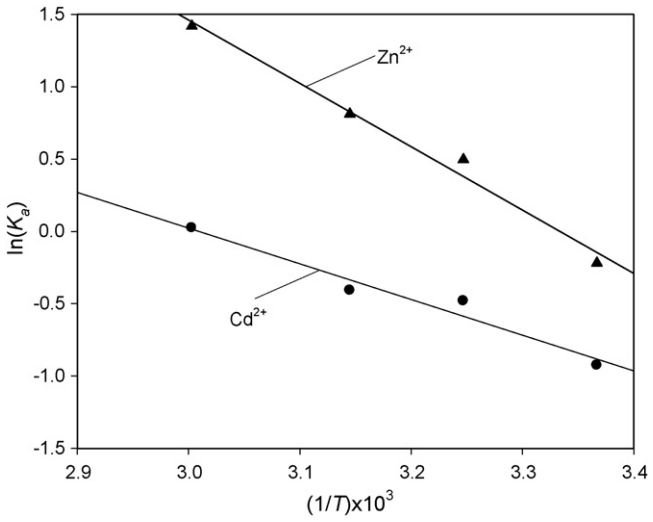

Fig. 15. Equilibrium constant plots.

upon the initial solute concentration, the Langmuir adsorption capacity given by q_m is independent of solution concentration. The results clearly indicate the affinity and preferential sorption behaviour of PSH towards Zn^{2+} as compared to Cd^{2+}. This is an interesting observation that may be explained in the light of a higher ionic potential of Zn^{2+} (5.33) compared to Cd^{2+} (4.2) [40]. Although both the cations have the same charge, Zn^{2+} has a smaller ionic radius (0.072 nm) than Cd^{2+} (0.096 nm) [40], and consequently a higher ionic potential. In spite of having the same hydration number of 6 in an aqueous solution, the larger ionic potential and charge density of zinc are responsible for the enhanced electrostatic attraction and binding at the active sites of the adsorbent surface. It will be interesting at this point to calculate the surface coverage on the basis of ionic size and the Langmuir maximum adsorption capacity (q_m). The sizes of the hydrated cations, that exist in an aqueous solution, are larger—0.43 nm for Zn^{2+} and 0.419 for Cd^{2+} [41], and the corresponding theoretical surface coverage values are 65.7 m^2/g for zinc and 35.3 m^2/g for cadmium. Since adsorption of the cations occurs at the active sites alone and does not cover the whole surface uniformly, this theoretical coverage appears reasonable in respect of the BET surface area of the adsorbent. Also the monolayer adsorption capacities for Cd^{2+} and Zn^{2+} metal ions are comparable with other agricultural-based adsorbents [12,32,36,41–49].

3.8. Effect of solution pH, particle size and temperature on the adsorption capacity of PSH from Langmuir isotherm

Langmuir adsorption capacity for both metal ions was determined for different particle size of the adsorbents, temperature and pH (Table 6). From the table it can be seen that with the change in pH from 3 to 6 the adsorption of Cd^{2+} increased from 2.1805 to 11.9048 mg/g and the adsorption of Zn^{2+} on PSH surface increased from 5.9737 to 15.128 mg/g at 24 °C with 0.6 mm particle size of PSH. The adsorption of both Cd^{2+} and Zn^{2+} decreased with the increase in the particle size of PSH. The Langmuir adsorption capacity (q_m) is plotted against particle size ratio or relative particle size in Fig. 14, which shows a sharp fall on q_m with increasing size of the adsorbent particles. This is expected on the basis of decreasing accessibility of the adsorption sites as the particle size goes up. The variation of q_m with pH is also shown in Fig. 14. The pattern of variation is about the same for both Cd^{2+} and Zn^{2+}. This can again be explained by the occurrence of an increasing number of negatively charged sites with increasing pH or decreasing acidity.

The Langmuir adsorption capacity also increases with temperature (Table 6). However, in order to have a quantitative estimate of the temperature effect and the relevant thermodynamic parameters we have calculated the adsorption equilibrium constant (K_a) at four different temperatures keeping the other parameters unchanged. The equilibrium constant is calculated from Eq (13).

The equilibrium constant is related to the free energy and entropy changes as well as the heat of adsorption by Eq. (15). It is reasonable to assume that the thermodynamic quantities to remain constant over the range of temperature under consideration. Then a plot of $\ln K_a$ against $1/T$ should yield a straight line that allows calculation of ΔH and ΔS from the slope and the intercept of such a plot. Fig. 15 shows the plot of the adsorption equilibrium constants for both Cd^{2+} and Zn^{2+}. The experimental values of K_a and the calculated values of the thermodynamic quantities are presented in Table 7. The adsorption process for both the cations is endothermic as indicated by the positive values of the heat of adsorption. The free energy change is negative as is expected for a spontaneous process but the entropy change is positive. The positive entropy change is indicative of the orderly arrangement of the species upon adsorption on the surface. The heat of adsorption values and the applicability of the Langmuir model indicate chemisorptions of the metal ions at the active sites.

3.9. Comparison of adsorption capacity (q_m) for Cd^{2+} and Zn^{2+} with other adsorbents

The adsorption capacities of PSH towards Cd^{2+} and Zn^{2+} have been compared with other adsorbents reported in the literature (Tables 8 and 9). For Zn^{2+} on PSH, comparison has been made with

Table 7
Calculated thermodynamic parameters for adsorption.

Temperature (°C)	K_a		ΔG (kJ/mol)		ΔH (kJ/mol)		ΔS (J/mol)	
	Cd^{2+}	Zn^{2+}	Cd^{2+}	Zn^{2+}	Cd^{2+}	Zn^{2+}	Cd^{2+}	Zn^{2+}
24	0.396	0.803	−8.8	−5.72	20.7	36.8	62	118
35	0.618	1.64						
45	0.665	2.25						
60	1.043	4.44						

Table 8
Comparison of adsorption capacities of various adsorbents for removal of Cd^{2+}.

No:	Adsorbents	Metal ions	Monolayer adsorption capacity (mg/g)	References
1.	Chitosan	Cd	5.93	[12]
2.	Peanut hull	Cd	5.96	[42]
3.	Corncorbs	Cd	8.89	[51]
4.	Bagasse fly ash	Cd	6.19	[35]
5.	Cornstarch	Cd	8.88	[51]
6.	Coffee husks	Cd	6.85	[43]
7.	Olive stone carbon	Cd	5.91	[45]
8.	Maize bran	Cd	7.43	[37]
9.	Olive Pomace	Cd	7.01	[52]
10.	Physic seed hull	Cd	11.89	Present work

rice husk ash [32], bagasse fly ash [35], peanut hull [42], coffee husk [43], cocoa shell [44], chitin [46], Turkish fly ashes [49] and coir [50]. For Cd^{2+} using PSH the comparison has been made with chitin [12], rice husk ash [32], bagasse fly ash [35], peanut hull [42], coffee husk [43], olive cake [45], juniper bark, juniper wood [47], hazelnut shell and almond shell [48]. The experimental values reported in the form of monolayer adsorption capacity were comparable to the values obtained by other workers under similar conditions.

3.10. Desorption studies

Desorption studies of metal ions were conducted to explore the possibility of recycling of PSH and recovery of the metal ions. Approximately 0.4 g of metal ions loaded PSH from the previous adsorption experiment was stirred with 50 mL of 0.1 M HCl solution for 24 h. The filtrate was analyzed for desorbed metal ions using Atomic Absorption Spectrophotometer. The same adsorbents were washed with distilled water for several times and the concentration of released metal ions form washing process was again analyzed. The concentration of desorbed metal ions corresponded to the amount of metal ions released form the sorbents. The total desorption for Cd^{2+} metal ions was 47% and for Zn^{2+} metal ions was 36%. The equilibrium adsorption data at different pH (e.g., Table 6) clearly show a reduction of uptake with decreasing pH. The acid solution (0.1 M HCl) used for desorption has a pH of 1. As such, the amount of metal ion (53% for Cd^{2+} and 64% for Zn^{2+}) retained in the PSH after acid treatment and partial elution of the metal represent the equilibrium adsorption at pH 1. We performed further experiments with stronger eluting acids. The desorption increased by about 10% but still incomplete. The percentage retention values for Cd^{2+} and Zn^{2+} was 47% and 59.5% for 1.0 M HCl, 50.4% and 43.8% for 0.2 M H_2SO_4, and 61.5% and 57.7% for 1.0 M H_2SO_4, in that order. Thus use of a stronger acid solution yielded marginally better elution at the cost of disintegration of the adsorbent. A complexing agent such as ETDA, tartaric acid or ethylene diamine is likely to be much more effective This will also be effective for recovery of the metals to compensate for the additional cost of the chemicals. A systematic work on it is in progress.

Table 9
Comparison of adsorption capacities of various adsorbents for removal of Zn^{2+}.

No:	Adsorbents	Metal ions	Monolayer adsorption capacity (mg/g)	References
1.	Chitin	Zn	5.79	[12]
2.	Rice husk ash	Zn	5.88	[32]
3.	Peanut hull	Zn	9.00	[42]
5.	Bagasse fly ash	Zn	7.03	[35]
6.	Shea butter seed husk	Zn	2.04	[54]
7.	Cork biomass	Zn	6.80	[55]
8.	Banana peel	Zn	5.80	[53]
9.	Orange peel	Zn	5.25	[53]
10.	Physic seed hull	Zn	12.29	Present work

4. Conclusions

PSH, an agro waste generated from plant-based oil industry, can be used as a potential low-cost adsorbent for the removal of Cd^{2+} and Zn^{2+} ions from the industrial effluents. It has been found that the amount of adsorption of Cd^{2+} and Zn^{2+} ions both increased with initial metal ion, temperature, amount of adsorbent, contact time, pH and smaller particle size of the adsorbent respectively. The rate of sorption of Cd^{2+} and Zn^{2+} was rapid for initial 2–10 min to take up the major part of the metal ions from the solution and the adsorption reached equilibrium after 3 h. Kinetic experiments indicate that adsorption of Cd^{2+} and Zn^{2+}on PSH followed a three-step processes comprising of an initial rapid adsorption stage, an intermediate slower adsorption stage and a final virtually no adsorption stage. It has also been confirmed by intra-particle diffusion model. The experimental results showed that Cd^{2+} and Zn^{2+}adsorption mechanism followed monolayer chemisorption, pseudo-second-order kinetics model and Langmuir isotherm model. Particle size of the adsorbent, solution pH and temperature had significant influence on the adsorption of both the ions by PSH. Under equilibrium condition 47% adsorbed Cd^{2+} and 36% adsorbed Zn^{2+} were desorbed from PSH. The monolayer adsorption capacity (q_m) of PSH was comparable with other reported agricultural-based adsorbents.

Appendix A.

Adsorption capacity, q_t (mg/g)

$$q_t = \frac{(C_i - C_t)V}{m} \quad (1)$$

Percentage removal

$$\%R = \frac{(C_i - C_t)}{C_i} \times 100 \quad (2)$$

where C_i (mg/L) and C_t (mg/L) are the concentration in the solution at time $t = 0$ and at time t, V is the volume of solution (L) and m is the amount of adsorbent (g) added.

Lagergren pseudo-first-order [13]

$$\log(q_e - q_t) = \log q_e - \frac{K_1}{2.303}t \quad (3)$$

Pseudo-second-order [9,13]

$$\frac{dq}{dt} = K_2(q_e - q_t)^2 \quad (4)$$

$$\frac{t}{q_t} = \frac{1}{K_2 q_e^2} + \frac{1}{q_e}t \quad (5)$$

$$h = K_2 q_e^2 \quad (6)$$

Intra-particle Diffusion Model [16]

$$q_t = K_{id}t^{0.5} + C \quad (7)$$

Freundlich isotherm [14,15]

$$\ln q_e = \ln K_f + \frac{1}{n}(\ln C_e) \quad (8)$$

Langmuir isotherm [17]

$$\frac{1}{q_e} = \left(\frac{1}{K_L q_m}\right)\frac{1}{C_e} + \frac{1}{q_m} \quad (9)$$

Dimensionless constant separation factor R_L [39];

$$R_L = \frac{1}{1 + K_L C_0} \quad (10)$$

Dubinin–Radushkevich isotherm [47,48,49]

$$\ln q_e = \ln X_m - \beta\varepsilon^2 \quad (11)$$

Polanyi potential of adsorption [47,48]

$$\varepsilon = RT \ln \frac{1}{C_e} \quad (12)$$

Mean free energy of adsorption [47,48]

$$E = (2\beta)^{-1/2} \quad (13)$$

Calculation of adsorption equilibrium constant

$$K_a = \frac{(q_t)_{250}}{C_e} \quad (14)$$

where $(q_t)_{250}$ is the amount adsorbed after 250 min of contact (which is sufficient for attainment of equilibrium as stated before) and C_e is the metal ion concentration (i.e., the equilibrium concentration of the solution) at that time.

Dependence of equilibrium constant on temperature

$$\ln K_a = \frac{-\Delta G}{RT} = -\frac{\Delta H - T\,\Delta S}{RT} \quad (15)$$

References

[1] M. Minceva, L. Markovska, V. Meshko, Removal of Zn^{2+}, Cd^{2+} and Pb^{2+} from binary aqueous solution by natural zeolite and granulated activated carbon, Maced. J. Chem. Chem. Eng. 26 (2007) 125–134.
[2] T.K. Sen, M.V. Sarzali, Removal of cadmium metal ion (Cd^{2+}) from its aqueous solution by aluminium oxide (Al_2O_3): a kinetic and equilibrium study, Chem. Eng. J. 142 (2008) 256–262.
[3] A.K. Bhattacharya, S.N. Mandal, S.K. Das, Adsorption of Zn^{2+} from aqueous solution by using different adsorbents, Chem. Eng. J. 123 (2006) 43–51.
[4] T.K. Naiya, P. Chowdhury, A.K. Bhattacharya, S.K. Das, Saw dust and neem bark as low-cost natural biosorbent for adsorptive removal of Zn^{2+} and Cd^{2+} ions from aqueous solutions, Chem. Eng. J. 148 (2009) 68–79.
[5] D. Mohan, K.P. Singh, Single and multi-component adsorption of cadmium and zinc using activated carbon derived from bagasse-an agricultural waste, Water Res. 36 (2002) 2304–2318.
[6] S. Larous, A.H. Meniai, M.B. Lehocine, Experimental study of the removal of copper from aqueous solutions by adsorption using sawdust, Desalination 185 (2005) 483–490.
[7] C. Zhu, Z. Luan, Y. Wang, X. Shau, Removal of cadmium from aqueous solution by adsorption on granular red mud 9GRM, Sep. Purif. Technol. 57 (2007) 161–169.
[8] A.B. Perez-Marin, V. Meseguer Zapata, J.F. Ortuno, M. Aguilar, J. Saez, M. Llorens, Removal of cadmium from aqueous solutions by adsorption onto orange waste, J. Hazard. Mater. B139 (2007) 122–131.
[9] G. McKay, Use of Adsorbents for the Removal of Pollutants from Wastewaters, CRC Press, Boca Raton, 1996.
[10] D.O. Cooney, Adsorption Design for Wastewater Treatment, Lewis Publishers, Boca Raton, 1998.
[11] A. Gurses, C. Dogar, M. Yalcin, M. Ac1ky1ldiz, R. Bayrak, S. Karaca, The adsorption kinetics of the cationic dye, methylene blue, onto clay, J. Hazard. Mater. 131 (2005) 217–228.
[12] B. Benguella, H. Benaissa, Cadmium removal from aqueous solutions by chitin: kinetic and equilibrium studies, Water Res. 36 (2002) 2463–2474.
[13] S. Lagergren, About the theory of so-called adsorption of soluble substances, in: Kungliga Svenska Vetenskapsakademiens, Handlingar Band 24, No. 4, 1898, pp. 1–39.
[14] A.W. Adamson, Physical Chemistry of Surfaces, 2nd ed., Interscience Publishers Inc., New York, 1967.
[15] H. Freundlich, Colloid and Capillary Chemistry, Metheun, London, 1926.
[16] W.J. Weber, J.C. Morris, Kinetics of adsorption on carbon from solution, J. Sanit. Eng. Div. Am. Soc. Civ. Eng. 89 (1963) 31–60.
[17] I. Langmuir, The Adsorption of Gases on Plane Surfaces of Glass, Mica, and Platinum, J. Am. Chem. Soc. 40 (1918) 1361–1403.
[18] M.M. Rao, A. Ramesh, G.P.C. Rao, K. Seshaiah, Removal of copper and cadmium from the aqueous solutions by activated carbon derived from Ceiba pentandra hull, J. Hazard. Mater. B129 (2006) 123–129.
[19] M.J. Horsfall, A.I. Spiff, Equilibrium sorption study of Al^{3+}, Co^{2+} and Ag^{+} in aqueous solutions by fluted pumpkin (Telfairia Occidentalis Hook f.) waste biomass, Acta Chim. 52 (2005) 174–181.
[20] Y.S. Ho, C.T. Huang, H.W. Huang, Equilibrium sorption isotherm for metal ions on tree fern, Process Biochem. 37 (2002) 1421–1430.
[21] M.M. Dubinin, L.V. Radushkevich, Equation of the characteristic curve of activated charcoal, Proc. Acad. Sci. USSR 55 (1947) 331–333.
[22] J. Medham, R.C. Denny, J.D. Barnes, M. Thomas, Vogel's Textbook of Quantitative Chemical Analysis, 5th ed., Pearson Education, Harlow, 2000.
[23] A.C. Lua, T. Yang, Characteristics of activated carbon prepared from pistachio-nut shell by zinc chloride activation under nitrogen and vacuum conditions, J. Colloid Interface Sci. 290 (2005) 505–513.
[24] V. Gomez-Serrano, J. Pastor-Villegas, A. Perez-Florindo, C. Duran-Valle, C. Valenzuela-Calahorro, FT-IR study of rockrose and of char and activated carbon, J. Anal. Appl. Pyrolysis 36 (1996) 71–80.
[25] S.B. Lalvani, A. Hubner, T.S. Wiltowski, Metal removal from process water by lignin, Environ. Technol. 18 (1997) 1663–1668.
[26] T.J. Barton, L.M. Bull, W.G. Klemperer, D.A. Loy, B. McEnaney, M. Misono, P.A. Monson, G. Pez, G.W. Scherer, J.C. Vartuli, O.M. Yaghir, Tailored porous materials, Chem. Mater. 11 (1999) 2633–2656.
[27] A.A. Abia, E.D. Asuquo, Lead (II) and nickel (II) adsorption kinetics from aqueous metal solutions using chemically modified and unmodified agricultural adsorbents, Afr. J. Biotechnol. 5 (16) (2006) 1475–1482.
[28] A. Marcilla, M.I. Beltrán, R. Navarro, Application of TG/FTIR to the study of the regeneration process of HUSY and HZSM5 zeolites, J. Therm. Anal. Calorim. 87 (2007) 325–330.
[29] T. Karthikeyan, S. Rajgopal, L.R. Miranda, Chromium (VI) adsorption from aqueous solution by Hevea brasilinesis saw dust activated carbon, J. Hazard. Mater. B124 (2005) 192–199.
[30] E.R. Alley, Water Quality Control Handbook, vol. 8, McGraw Hill, 2000, pp. 125–141.
[31] C.K. Jain, Adsorption of zinc onto bed sediments of the river Ganga: adsorption models and kinetics, Hydrol. Sci. J. des Sci. Hydrologiques 46 (2001) 419–434.
[32] V.C. Srivastava, I.D. Mall, I.M. Mishra, Removal of cadmium(II) and zinc(II) metal ions from binary aqueous solution by rice husk ash, Colloids Surf. A: Physicochem. Eng. Aspects 312 (2008) 172–184.
[33] D. Mohan, C.U. Pittman Jr., M. Bricka, F. Smith, B. Yanceyd, J. Mohammad, P.H. Steele, M.F. Alexandre-Franco, V. Gómez-Serrano, H. Gong, Sorption of arsenic, cadmium, and lead by chars produced from fast pyrolysis of wood and bark during bio-oil production, J. Colloid Interface Sci. 310 (2007) 57–73.
[34] R.T. Daher, Trace metals (lead and cadmium exposure screening), Anal. Chem. 67 (1995) 405–410.
[35] V.C. Srivastava, I.D. Mall, I.M. Mishra, Modelling individual and competitive adsorption of cadmium (II) and zinc (II) metal ions from aqueous solution onto bagasse fly ash, Sep. Sci. Technol. 41 (2006) 2685.
[36] C.F. Baes, E.M. Robert, The Hydrolysis of Cations, Wiley, New York, 1976.
[37] Y. Önal, C. Akmil-Basar, D. Eren, C. Sarıcı-Ozdemir, T. Depci, Adsorption kinetics of malachite green onto activated carbon prepared from TunC, bilek lignite, J. Hazard. Mater. 128 (2006) 150–157.
[38] K.R. Hall, L.C. Eagleton, A. Acrivos, T. Vermeulen, Pore and solid diffusion kinetics in fixed-bed adsorption under constant-pattern conditions, I & EC Fundam. 5 (1966) 212–223.
[39] D.J. Shaw, Introduction to Colloid and Surfaces Chemistry, Butterworth-Heinemann, Oxford, 1992, Chapter 6.
[40] U.K. Saha, S. Taniguchi, K. Sakurai, Simultaneous adsorption of cadmium, zinc and lead on hydroxyaluminum and hydroxyaluminosilicate-montmorillonite complexes, Soil Sci. Soc. Am. J. 66 (2002) 117–128.
[41] E. Demirbas, N. Dizge, M.T. Sulak, M. Kobya, Adsorption kinetics and equilibrium of copper from aqueous solutions using hazelnut shell activated carbon, Chem. Eng. J. 148 (2009) 480–487.
[42] P. Brown, I.A. Jefcoat, D. Parrish, S. Gill, E. Graham, Evaluation of the adsorptive capacity of peanut hull pellets for heavy metals in solution, Adv. Environ. Res. 4 (2000) 19–29.
[43] W.E. Oliveira, A.S. Franca, L.S. Oliveira, S.D. Rocha, Untreated coffee husks as biosorbents for the removal of heavy metals from aqueous solutions, J. Hazard. Mater. 152 (2008) 1073–1081.
[44] N. Meunier, J. Laroulandie, V.F. Blais, R.D. Tyagi, Cocoa shells for heavy metal removal from acidic solutions, Bioresour. Technol. 90 (2003) 255–263.
[45] S.A. Doyurum, Çelik, Pb(II) and Cd(II) removal from aqueous solutions by olive cake, J. Hazard. Mater. B138 (2006) 22–28.
[46] B. Benguella, H. Benaissa, Effects of competing cations on cadmium biosorption by chitin, Colloids Surf. A: Physicochem. Eng. Aspects 201 (2002) 143–150.
[47] E.W. Shin, K.G. Karthikeyan, M.A. Tshabalala, Adsorption mechanism of cadmium on juniper bark and wood, Bioresour. Technol. 98 (2007) 588–594.
[48] Y. Bulut, Z. Tez, Adsorption studies on ground shells of hazelnut and almond, J. Hazard. Mater. 149 (2007) 35–41.
[49] B. Bayat, Comparative study of adsorption properties of Turkish fly ashes. I. The case of nickel(II), copper(II) and zinc(II), J. Hazard. Mater. B95 (2002) 251–273.
[50] K. Conrad, H.C.B. Hansen, Sorption of zinc and lead on coir, Bioresour. Technol. 98 (2007) 89–97.
[51] R. Zacaria, C. Gerente, Y. Andres, P.L. Cloirec, Adsorption of several metal ions onto low cost biosorbents: kinetic and equilibrium studies, Environ. Sci. Technol. 36 (2002) 2067–2073.
[52] M.A. Ferro-Garcia, J. Rivera-Utrilla, J. Rodriguez-Gordillo, I. Bautista-Toledo, Adsorption of zinc, cadmium and copper on activated carbon obtained from agricultural byproducts, Carbon 26 (1988) 363–373.
[53] G. Annadurai, R.S. Jung, D.J. Lee, Adsorption of heavy metals from water using banana and orange peels, Water Sci. Technol. 47 (2003) 185–190.
[54] I.C. Eromosele, L.D. Abare, Sorption of iron and zinc ions from non-aqueous solution by shea butter (*Butyrospermum parkii*) seed husks, Bioresour. Technol. 66 (1998) 129–132.
[55] N. Chubar, J.M.R. Carvalho, M.J.N. Correia, Cork biomass as biosorbent for Cu(II), Zn(II), Ni(II), Colloids Surf. A: Physicochem. Eng. Aspects 230 (2003) 57–65.